 doi:10.20944/preprints201703.0060.v1

Article

Biomass-Derived, Interconnected and Reticular Carbon Microtubes Electrodes for Symmetric Capacitors

Nannan Wang [1,2], Ning Zhang [3], Wutao Wei [1], Shizhong Cui [1], Hongwei Hou [2], Guangshan Zhu [3], Weihua Chen [2,*] and Liwei Mi [1,*]

[1] Center for Advanced Materials Research, Zhongyuan University of Technology, Zhengzhou 450007, China; wangnn989@163.com (N.W.); weiwutaozut@163.com (W.W.); liwei_mi@zut.edu.cn (S.C.)
[2] College of Chemistry and Molecular Engineering, Zhengzhou University, Zhengzhou 450001, China; houhongw@zzu.edu.cn
[3] State Key Lab of Inorganic Synthesis & Preparative Chemistry, Jilin University, Changchun 130012, China; mlwxcu@163.com (N.Z.); zhugs@jlu.edu.cn (G.Z.)
* Correspondence: chenweih@zzu.edu.cn (W.C.); mlwzzu@163.com (L.M.)

Abstract: Biomass materials have received attention for energy storagebecaused of the advantage of low-cost, easy-to-prepare, and eco-friendliness. Three-dimensional carbon materialswith abundant pore structure gradually becomeresearch hotspot in high-performance energy storage. In this study, an easy-to-prepare, green, light and elastic activated carbon was present using the biomass *Juncus effusus* (JCE) via high-temperature pyrolysis, followed by activation in air. Compared with previously reported bio-carbons, the proposed air-activated bio-carbon contributes in the fabrication of pores to preserve the interconnected, reticular and tubular structure. Moreover, the interconnected porous material also inherits the excellent tenacity of the original JCE such as the material can be bended to below 90° under an external force while maintaining structural integrity. The activated porous carbon material exhibits an enhanced electric double-layer capacitance (~210 F g^{-1} at 1 A g^{-1}), with capacitance retention of ~78.62% at 10 A g^{-1}. The interconnected porous carbon microtubes electrode as a double-layer symmetric capacitor exhibits considerable capacitance retention (84%) after 2000 cycles at 1 A g^{-1}. The improved energy storage performance was proposed to be attributed to the shortened ionic diffusion distance and sufficient contact between the interface of the carbon electrode and electrolyte, which is resulted from the elastic, undamaged structure and types of pores. These results demonstrated that as-preparedcarbon materials have potentional application in symmetric capacitors.

Keywords: elasticbiomass; tubular structure; interconnected porous carbon; electric double layer capacitance

1. Introduction

Carbon materials with high surface area, accessible surface chemical, special diffusion pathway for ions, and easy-to-functionalize surface have attracted much attention in various fields, such as chemical adsorption, electrocatalysis, energy storage, electrochemical senor, and capacitor devices [1–6]. Carbon materials for these advanced applications should essentially possess an appropriate structure to allow ion migration [7]. Carbon materials are especially used as electrodes in electrochemical double-layer capacitors (EDLCs) to store energy [8, 9].

Numerous studies have reported that special structures are often needed to obtain electrode materials with good performance. Typical supercapacitor electrode materials can be categorized into one-dimensional (1D), two-dimensional (2D), and three-dimensional (3D), depending on the structure for charge transfer. Some examples of these materials are carbon nanotubes [10–13], graphene [14–17], carbon nanofiber [18–20], and porous carbon [21, 22]. Tubular nanostructure offers high surface area with less utilization of mass to encapsulate materials with poor conductivity [23,

 doi:10.20944/preprints201703.0060.v1

24] but has low surface area [25] and high contact resistance at the electrode-current collector [26, 27]. Although 2D materials, such as graphene nanosheets, provide short diffusion distance and high flexibility [28, 29], graphene nanosheets tend to aggregate (self-restack) during the preparation of the electrode, resulting in substantial loss of active surface area and reduced electrochemical performance [28]. Developing multidimensional architectures of combined 1D and 2D structures which can provide efficient ion diffusion between electrode and electrolyte can reasonably solve these drawbacks [30]. Consequently, the overall performance of the capacitor can be improved. However, such materials are relatively expensive because of their complex preparation processes and scarce raw materials. These characteristics severely limit the potential of these carbon materials for large-scale production and practical application.

Compared with artificially synthesized 3D carbon material, carbon-based materials derived from biomass, a source of "green" and renewable energy, have also been demonstrated as better alternative for capacitor devices as positive and negative electrodes [31, 32]. Numerous types of biomass sources, such as cotton, celtuce leaves, and bamboo, have been used to improve performance by manufacturing porous structure and building 3D framework [33–38]. Chemical and physical activation are two common methods for fabricating pores to optimize the structure and improve corresponding application performance. Macroporous, mesoporous, and microporous structures usually present enhanced electrochemical performance compared with that of the single-sized pore materials. Thus, different nanoscale pores can minimize the diffusion distance to the interior surface and lower resistance to facilitate energy storage [39]. Moreover, surface functional groups containing oxygen, nitrogen, fluorine, phosphorus, and other heteroatoms can considerably enhance the capacitance of carbon electrode because of the pseudocapacitance effect in charge or mass transfer between electrodes and electrolytes [40–42]. Carbon oxidation is the most straightforward way to generate oxygen groups on the carbon surface. However, these oxygen groups are unstable during cycling, leading to the fading of the pseudocapacitance [43]. Li et al. [44] found that the performance of activated carbon in air at 300 °C (AC-air) was better than that of AC-KOH, because AC-air contained more nitrogen content but with similar oxygen content. Introducing nitrogen into the electrode materials can enhance electrical conductivity and wettability for high pseudocapacitance [45]. In addition, materials with high tenacity have been used for devices to store and convert energy [46]. The reported bio-carbon electrodes have low elasticity. These carbon sources generally show poor mechanical stability and lead to mass reduction and partial destruction of the pristine microstructure under high-temperature pyrolysis. These processes decrease specific capacitance, limiting the application of bio-carbons [47, 48]. Thus, the development of a highly elastic carbon material remains a significant challenge.

In this study, we present a low-cost, green, light and high elastic bio-carbon derived from *juncus effuses* which is throughout the warm region of the world, which can be harvested for mass production in the fall of the year. Compared with other biomass, the natural biomass is easy to production and has special 3D tubular structure. After air-activation, the porous tubular bio-carbon can be obtained (Figure 1). The as-obtained porous carbon material inherited the good flexibility of the original biomass with high tenacity. The porous carbon material after being assembled as a symmetric capacitor exhibited enhanced electric double-layer capacitance (~210 F g^{-1} at 1 A g^{-1}), with capacitance retention of ~78.62% at 10 A g^{-1}. Moreover, the carbon microtubes electrode exhibited considerable capacitance retention (84%) after over 2000 cycles at 1 A g^{-1} as a double-layer symmetric capacitor. Therefore, the porous and reticular carbon is highly promising for various applications, especially, in energy storage.

Preprints (www.preprints.org) | NOT PEER-REVIEWED | Posted: 13 March 2017 doi:10.20944/preprints201703.0060.v1

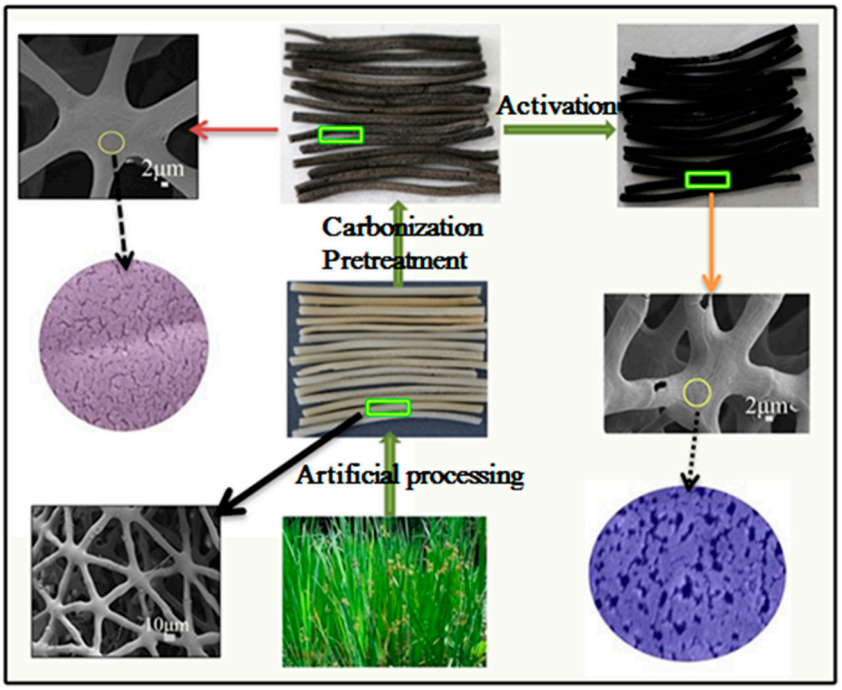

Figure 1. Schematic illustration of the Carbons fabrication.

2. Results and Discussion

Morphology and structure.*Juncus effusus* (JCE) is a crude herb with remarkable tenacity and grid tubular structure. Compared with other biomasses, this biomass is easy to bend and has no deformation. Its tenacity is still maintained after carbonization, and its tubular structure is not destroyed readily. This flexible biomass is composed of amino acids, which contain abundant nitrogen. Thus, this plant is chosen as a carbon source containing nitrogen with 3D flexible network. The carbonized JCE with high tenacity possessed an interconnected tubular framework with slight inorganic impurities. Heat treatment at 300 °C for 8 h in air was performed to ensure the removal of impurities and produce pores to increase surface area to provide new electronic transmission channels. The overall changes in the bio-carbon materials under different sintering processes are shown in Figure 2. High-temperature pyrolysis provided the condition for fabricating pores. The resulting physical and chemical changes gradually increased the pores on the surface, which is conducive for storing ions and electrons.

Preprints (www.preprints.org) | NOT PEER-REVIEWED | Posted: 13 March 2017 doi:10.20944/preprints201703.0060.v1

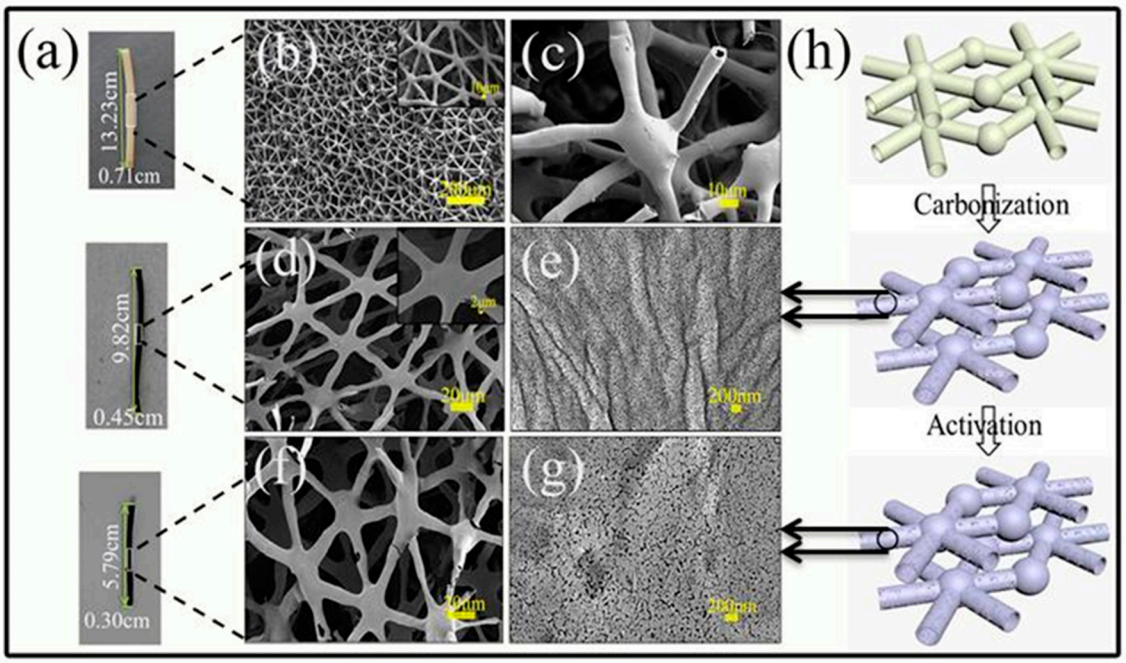

Figure 2. (**a**) Digital photographs of the length and width of JCEs; (**b, c**) SEM images of the original JCE with low and high magnification; (**d, e**) the JCE-1 sample with low and high magnification; (**f, g**) the JCE-2 sample with different magnification; (**h**) schematic illustration of the surface changes before and after activation.

Figure 2a exhibits the volumetric change after different stages, which reveal that the annealing process induced the shrinkage of the bio-carbon. However, the three frameworks shown in the scanning electron micrographs in Figures 2b, d and f were not damaged. The structure of the unprocessed original JCE shows an interconnected hollow tubular structure in an orderly arrangement, and no pore was found on its surface (Figures 2b and c). Such hollow 3D structure can not only enhance the contact between the electrode material and electrolyte, but also serve as a reservoir for the electrolyte, shortening the ion diffusion pathway and facilitating charge transfer. Figure 2d exhibits the image of JCE-1, which inherited the interconnected tubular structure. In addition, pores gradually formed on the framework of JCE-1 (Figure 2e). Such morphological change should be associated with carbon loss upon high-temperature carbonization. The surface microconvexities which resembled the texture of a tree may be ascribed to the shrinkage degree of material during annealing. Figure 2f reveals that JCE-2 retained the overall structural integrity. Nevertheless, compared with the carbon material without activation, some pores of JCE-2 were entirely opened, and different nanoscale pores were generated on JCE-2 as observed at high magnification (Figure 2g). These findings suggest the effectiveness of the proposed activation method to create porosity on the network. Figure 2h presents schematic illustration of the surface changes before and after activation.

Digital photographs of the bio-carbons which indicate the tenacity before and after carbonization are shown in Figures 3I and II to investigate whether the structure of JCE was damaged under an external force. The original JCE was bended to different angles, and fracturing of the surface, even at 60°, was not observed. The activated carbon also retained good flexibility after carbonization. However, tenacity was destroyed when JCE was bended to below 90°, because carbonization destroys some chemical bonds, consequently reducing elasticity. The activated carbon generally has good flexibility, which endows great application potential.

Preprints (www.preprints.org) | NOT PEER-REVIEWED | Posted: 13 March 2017 doi:10.20944/preprints201703.0060.v1

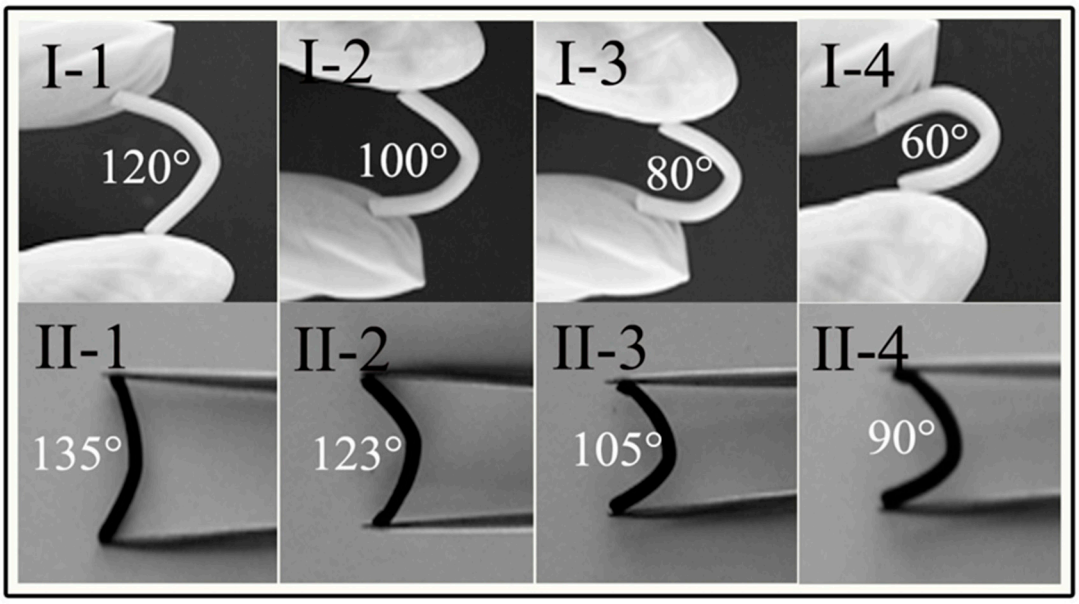

Figure 3. Digital photographs of the original JCE (**I**) and JCE-2 (**II**) for the tenacity.

The structure and composition of JCE-1 and JCE-2 samples were further investigated by X-ray diffraction (XRD) and energy dispersive spectroscopy. Figure 4a shows the XRD patterns of the two samples. The diffraction peaks at 23.64° and 38.18° could be indexed to the (002) and (100) peaks of graphitic carbon. These two peaks became weaker and broader after activation, indicating the formation of amorphous carbon. Figure 4b exhibits that the atomic ratios of C:O were 95.13:2.67 and 90.58:8.01, respectively. Only ~1.41 wt% N was detected in the JCE-2 and ~1.37 wt% N in JCE-1. The oxygen contents increased slightly after activation in air because bonding interaction occurred between carbon and oxygen at 300 °C in air. The bonding altered the functional groups on the surface of the material and improved performance. In addition, compared with JCE-1, the loss of carbon in JCE-2 further reveals the transformation of microporous and mesoporous structures. Figure 4c reveals the type-IV isotherm with clear H2-type hysteresis loops in the relative pressure region of 0.5–1.0 P/P_0. The occurrence of capillary condensation indicates the wide distribution of pore sizes, which are consistent with the scanning electron microscopy results. The BET and Langmuir surface areas of JCE-2 were 1362 and 1695 $m^2 g^{-1}$, respectively. The total pore volume of JCE-2 was 0.87$cm^3 g^{-1}$, which was smaller than those of previously reported bio-carbons. Figure 4d indicates that the pores on the network had primarily small size distribution, which was calculated from adsorption branch as ~3.9 and ~2.1 nm, respectively. The BET result indicates that the structure isa mesoporous structureclose to the micropore one. This structure could shorten the diffusion pathway of ion and facilitated ion transport, which would further improve the performance of activated carbon.

Preprints (www.preprints.org) | NOT PEER-REVIEWED | Posted: 13 March 2017 doi:10.20944/preprints201703.0060.v1

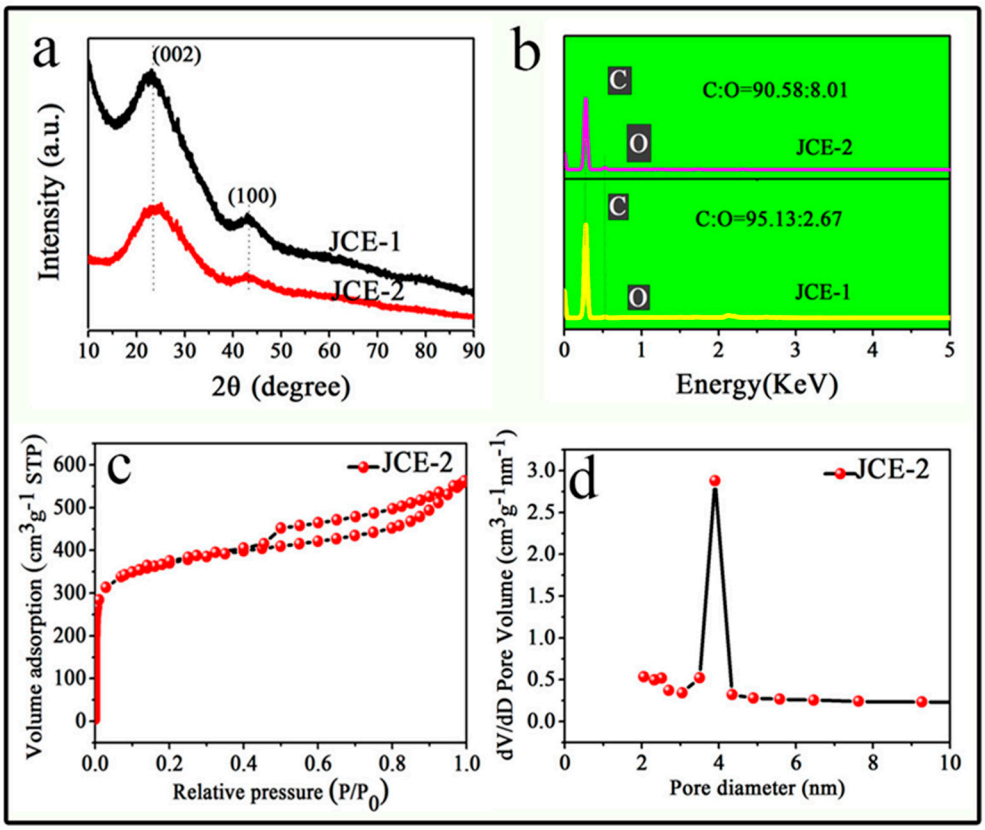

Figure 4. (**a**) XRD pattern and (**b**) EDX spectrum of JCE-1 and JCE-2; (**c**) Nitrogen adsorption-desorption isotherm and (**d**) pore-size distribution of JCE-2.

Electrochemical Measurements The part of hollow tubular structure can be preserved because of the flexible properties of bio-carbon. This structure can help the electron and ion transfer to store energy. Figure 5a shows that the CV curves of JCE-2 from -1.0 to 0 V demonstrates the regular rectangle, which suggests that the capacitive response of electrical double-layer formation and redox reaction, which may be attribute to surface oxygen and nitrogen functionalities. Figure 5b shows the galvanostatic charge/discharge (GCD) curves at different current densities, exhibiting symmetric charge-discharge curves with small IR drop. The high specific capacitance of 260 F g^{-1} was obtained for JCE-2 at a current density of 0.5 A g^{-1}. The value is higher than most of bio-carbon. Moreover, the synthesized product still retained high specific capacitance of 218 F g^{-1} (~84% capacitance retention) at a current density of 10 A g^{-1}. The high results reveal that the porous 3D material provides storage environment for ions and electrons. Simultaneously, the introduction of oxygen and nitrogen accelerate the migration velocity of electrons, improving the performance, especially for the rate capability.

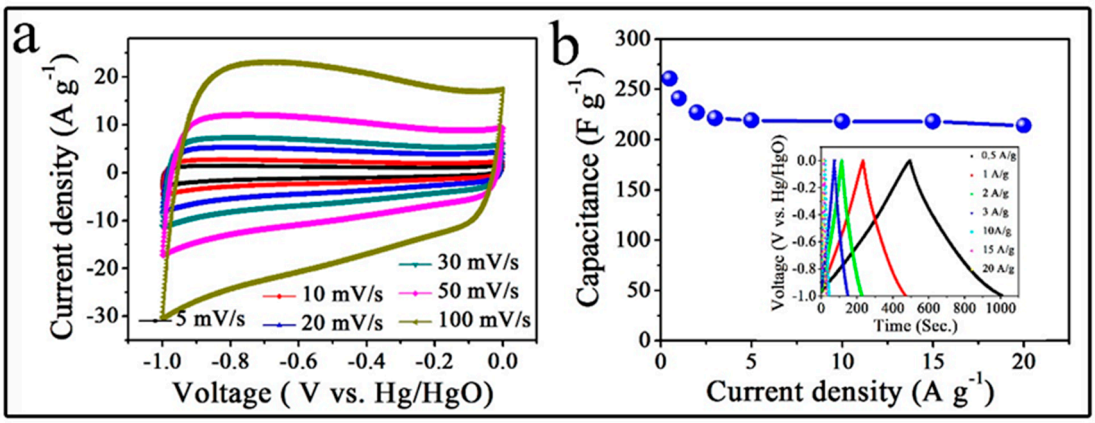

Preprints (www.preprints.org) | NOT PEER-REVIEWED | Posted: 13 March 2017 doi:10.20944/preprints201703.0060.v1

Figure 5. (**a**) CV curves as a function of discharge current density and (**b**) GCD curves and specific capacitances of JCE-2 at different densities in a three-electrode cell.

To explore the practical applications of the JCE for capacitor, symmetric devices were assembled. The related capacitive performances with JCE-based electrodes were also evaluated. Figure 6a shows the CV curves of JCE-2//JCE-2 symmetric cell in the voltage windows of 0.9, 1.0, 1.2, and 1.3 V at the scan rate of 10 mV/s. All curves exhibit rectangle-like shapes, while polarization began to increase gradually when the operation voltage was extended to over 1.2 V. However, polarization was larger at the working voltage of 1.0 V (Figure S1). Therefore, 0.9 V was determined as the optimal voltage for subsequent measurements. Figures 6b and 6c show the CV curves of JCE-1//JCE-1 and JCE-2//JCE-2 symmetric cells with potential window from 0 V to 0.9 V in 2 M KOH aqueous solution at different scan rates ranging from 10 mV s^{-1} to 100 mV s^{-1}. Fig. 6b displays that the rectangular-shaped CV curves of JCE-1//JCE-1 symmetric system and the slight distortion at the high scan rates suggest that the JCE-1 works as an EDLC. Figure6c exhibits that the JCE-2//JCE-2 cell exhibits perfect rectangle-like shapes, indicating a capacitance response derived from the EDLC with stable reversibility and good performance. The CV area of the JCE-2//JCE-2 cell is much larger than that of the JCE-1//JCE-1 cell, suggesting that the symmetric system of JCE-2//JCE-2 performs better because of the easier accessibility of ion along its porous pathways. Figure6d reveals the relationship between specific capacitances and sweep rates of the two cells. The specific capacitance of JCE-2//JCE-2 cell was 53 F g^{-1} at 5 mV s^{-1}, and the cell retained 42.84 F g^{-1} even at a high sweep rate of 50 mV s^{-1} with a capacitance retention ration of 80% (Figure6e). However, the capacitance of JCE-1//JCE-1 was only 50% that of JCE-2//JCE-2, which demonstrated that the soft and open porous structure via activation in air helpedto improve the performance of carbon materials.

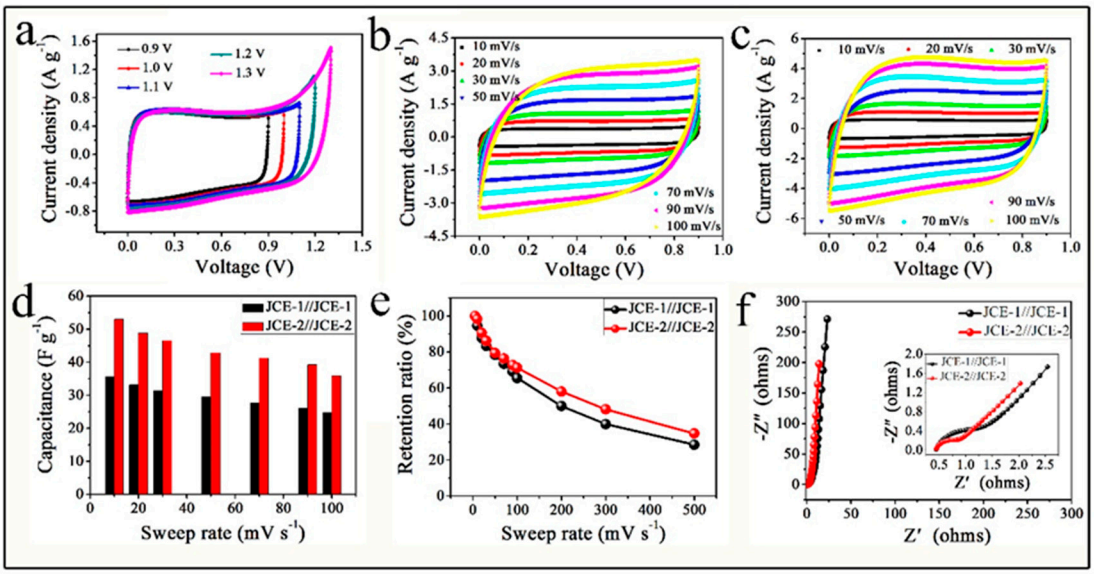

Figure 6. Electrochemical performance of the cells for carbons: Cyclic voltammograms (CV) curves of (**a**) JCE-2//JCE-2 at different potential windows; (**b**) JCE-1//JCE-1 and (**c**) JCE-2//JCE-2 at different sweep rates; (**d**) specific capacitances; (**e**) capacitance retention ratios and (**f**) Nyquist plots of JCE-1//JCE-1 (black) and JCE-2//JCE-2 (red).

The electrochemical impedance spectra of the materials were characterized to further investigate the behavior of the assembled symmetric systems. Similar shapes with a straight line at low frequency and a half arc at the high-frequency region were observed (Figure6f). The high-frequency shape could be ascribed to the double-layer capacitance (C_{dll}) and charge transfer resistance (R_{ct}) between the electrode and electrolyte interface. The inclined line is due to the Warburg impedance in the low-frequency region, resulting from the frequency dependence of ion transport in the electrolyte. The JCE-2//JCE-2 cell presented smaller interfacial charge transfer impedance in KOH electrolyte, indicating improved charge diffusion velocity between electrolyte ions and active surface. The slopes

 doi:10.20944/preprints201703.0060.v1

of the Nyquist plots show that JCE-2//JCE-2 displays a more nearly vertical line than JCE-1//JCE-1, indicating a capacitive performance. JCE-2//JCE-2 with rich mesoporous structure exhibitsa lower impedance and more ideal capacitor behavior, corresponding to the CV curve.

The GCD curves exhibit a nearly symmetric triangular shape with an IR drop in Figure7a. Specific capacitances were calculated to be 131.4, 126.93, 122.93, 110.67, and 93.25 F $g^{-1}$from discharge times at different current densities of 0.5, 1, 3, 5, and 10 A g^{-1}, respectively. The IR drops at different currentdensities usually resulted from equivalent series of resistance. The IR increased gradually as the current density increased.The internal resistance may have beencaused by the ash from carbon materials. Meanwhile, Figure7b reveals the charge/discharge condition of JCE-2. Compared with JCE-1, the JCE-2 has a smaller IR drop, which may be ascribed to oxygen and nitrogen functionalities as well as the existence of mesoporous produced on the surface in the air-activation stage. In addition, the specific capacitances increased significantly. The activated JCE-2 exhibited considerable capacitance of 175.56 F g^{-1}, when the discharge current density was 10 A g^{-1}, with capacitance retention of ~78.62% (Figure 7c). As a reference, the bio-carbon was also chemically activated with KOH. Though all electrodes exhibit nearly symmetric profiles, it can be seen that the JCE-KOH electrode shows a lower capacitance than JCE-2 (Figure 7d, 7e). The specific capacitances for two electrodes at different current densities are collected in Table 1. The results demonstrate activation-KOH and activation-air both provide favorable condition for the diffusion and storage of ions and electrons, but, activation-air is more conducive to improve the capacitance of porous JCE. It is noticeable, JCE-2, despite its lower surface area, exhibitsa potential advantage as an electrode material for capacitor compared with the most bio-carbon activated in KOH (Table S1). Figure7f shows that the bio-carbon electrodes exhibit good cycling stability as double-layer symmetric capacitors. However, the capacitance retention of JCE-2 (84%) is not as good as that of JCE-1 (95%) after over 2000 cycles at 1 A g^{-1}. Figure S2 shows that the shape and area of the CV curves after 2000 cycles are nearly consistent by the first cycle, which may be ascribed to the oxygen groups produced on the surface in the air-activated process.

Preprints (www.preprints.org) | NOT PEER-REVIEWED | Posted: 13 March 2017 doi:10.20944/preprints201703.0060.v1

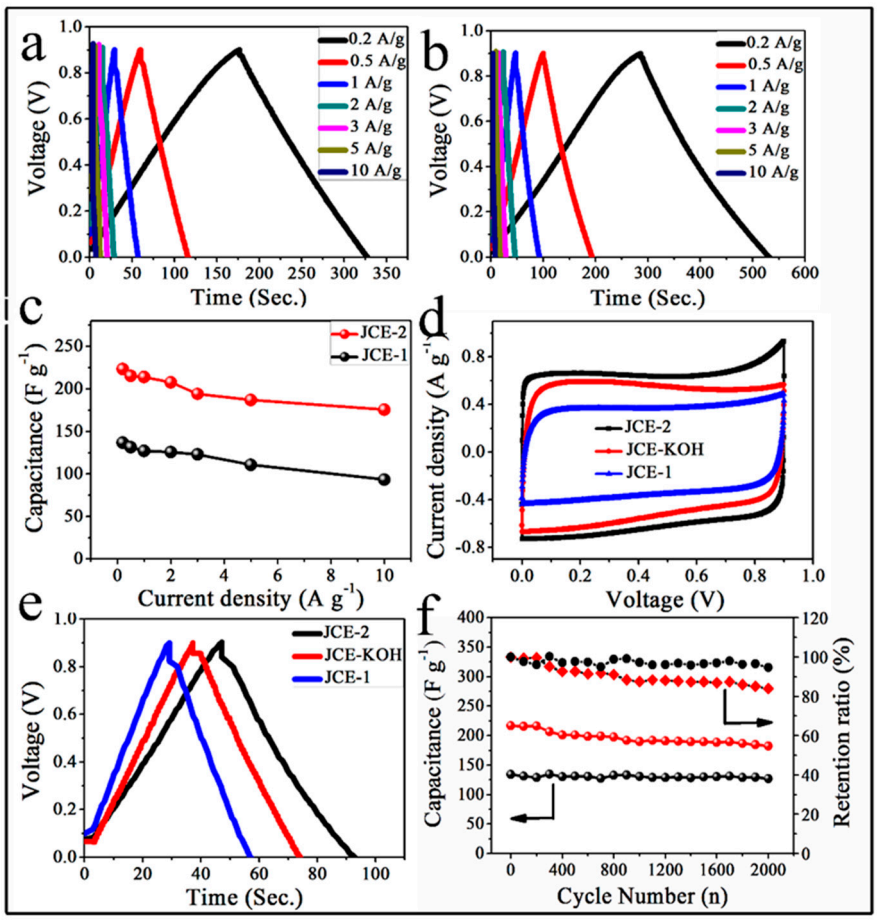

Figure 7. Electrochemical characteristics of single electrode for carbons: GCD curves of (**a**) JCE-1 and (**b**) JCE-2 at different current densities; (**c**) the specific capacitance as a function of discharge current density; (**d**) CV and (**e**) GCD curves of JCE-1, JCE-2, JCE-KOH at 10 mV s^{-1} and 1A g^{-1}, respectively; (**f**) cycling stability and capacitance retention of JCE-1 (black) and JCE-2 (red) at charge/discharge current density of 1 A g^{-1}.

Table 1. Comparison of the electrochemical performance in the two-electrode testing by different activation way for bio-carbon derived from JCE.

Samples	Activated Way	Specific Capacitance (F g-1)				Yield
		1 A g^{-1}	2 A g^{-1}	5 A g^{-1}	10 A g^{-1}	
JCE-2	Air	213	207	186	175	72%
JCE-KOH	KOH	180	171	165	150	43.44%

Results from the CV, galvanostatic charge/discharge curves, and cycling stability show that the hetero-atoms only play a role in electroconductivity, but have little contribution to the supply of capacitance during the charge/discharge process. Thus, the whole system is mainly an EDLC. The properties of pesudocapacitance should be exhibited by adjusting the quantity of hetero-atoms to further improve the performance of carbonized JCE.This section may be divided by subheadings. It should provide a concise and precise description of the experimental results, their interpretation as well as the experimental conclusions that can be drawn.

3. Materials and Methods

3.1. Preparation of activated carbon derived from Juncus effusus (JCE) with flexibility.

Preprints (www.preprints.org) | NOT PEER-REVIEWED | Posted: 13 March 2017 doi:10.20944/preprints201703.0060.v1

The JCE was bought and used without any further purification. The 0.1 g rushes was directly pyrolyzed at 900 °C for 2 h under Ar atmosphere to obtain the pyrolytic carbon material. After cooling down to room temperature, the samples were by ultrasound in KOH for 2 h, and then washed with HCl and DI water until PH reached a value of 7 (denoted as JCE-1). After drying at 80 °C for 12 h, JCE-1 was activated at 300 °C for 8 h in air at a heating rate of 5 °C min^{-1} to produce activated carbon (denoted as JCE-2). Meanwhile, KOH is used as chemical activation agent to gain JCE-KOH. Finally the three products were collected for further characterization.

3.2. Structural Characterization.

The morphologies and sizes of the as-prepared samples were determined by field-emission scanning electron microscopy (SEM) at an accelerating voltage of 5 kV with an energy-dispersive X-ray spectroscopy (EDX) system. X-ray diffraction (XRD) patterns were performed with a Bruker D8 Advance X-ray powder diffractometer using Cu-Kα irradiation within $10^{o} \leq 2\theta \leq 90^{o}$ at a scan rate of 4o min-1. Nitrogen adsorption/desorption measurements were performed to investigate the surface characteristics at 77 K on a Micromeritics ASAP2420 instrument. The Brunauer–Emmett–Teller (BET) method was utilized to calculate the specific surface area and the pore size.

3.3 Electrochemical Measurements.

The electrochemical measurements were carried out by two-electrode systems. The working electrode was prepared by mixing the as-prepared active carbons, acetylene black, PTFE with a mass ratio of 8:1:1 in an appropriate amount of isopropyl alcohol. After the solvent evaporated, this paste was pressed at 10 MPa and the electrode materials were dried for 12 h at 100 °C, then loaded 3~4 mg between two pieces of nickel foam under a pressure of 100 kPa. Then the two ~electrode cell was soaked in the 2 M KOH aqueous solution and waiting for test. Gravimetric capacitance from galvanostatic charge/discharge was calculated by using the formula：

$$C_{single\text{-}electrode}=4I\Delta t/m\Delta V \ (F/g) \quad (1)$$

$$C_{cell}= I\Delta t/m\Delta V \ (F/g) \quad (2)$$

The gravimetric specific capacitance of the individual electrode is calculated from the CV curve based on the following equation:

$$C_{cell}=A/(2sm\Delta V) \ (F/g) \quad (3)$$

Here, I is constant discharge current, Δt is the time period for a full discharge, A is the integral area of the closed CV curve, m is the mass of the active material, ΔV is width of the potential widow, s is the potential scan rate.

Cyclic voltammetry (CV) measurements were carried out on a CHI604E electrochemical workstation (Chenhua, Shanghai, China) at voltage scan rates ranging from 10 to 100 mV s-1 and the potential ranges from 0 to 0.9, 1.0, 1.2, and 1.3 V, respectively. The electrochemical impedance spectroscopy data were recorded using a electrochemical workstation for a frequency between 0.01 Hz and 100 kHz. The electrochemical galvanostatic charge/discharge measurements and cycling tests of the products were performed using an ordinary LAND testing system.

4. Conclusions

An interconnected and reticular carbon microtubes derived from elastic JCE was introduced by high-temperature carbonization and activation in air. The bio-carbon simultaneously inherited the interconnected tubular structure from the original JCE and produced rich mesopores on the surface, providing high SSA and a series of pore sizes. In addition, the porous carbon microtubes could be bended to below 90^{o}, without fracturing on the surface. The porous material with tubular structure, as a symmetric capacitor, exhibited enhanced electric double-layer capacitance (~210 F g^{-1} at 1 A g^{-1}), with capacitance retention of ~78.62% at 10 A g^{-1}, indicating considerable tenacity. The inactivated carbon electrode could also offer high specific capacitance of 126.93 F g^{-1}at 1 A g^{-1}. Moreover, the two bio-carbon electrodes exhibited considerable cycling stability. Thus, compared with chemical activation, the air-activated way can not only create positive effect for pore fabrication to improve

performance of bio-carbon for symmetry capacitor, but also preserves the integrity and tenacity of the framework.

Supplementary Materials: The following are available online at www.mdpi.com/link, Figure S1: CV curves of JCE-1//JCE-1 at different potential windows, Table S1: CV curves of JCE-2 // JCE-2 at the first, 1000th, 2000th cycle.

Acknowledgments: This work was supported by the National Natural Science Foundation of China (Grant No. 21671205 and U1407103), Collaborative Innovation Centre of Henan Textile and Clothing Industry, Innovation Scientists and Technicians Troop Construction Projects of Henan Province (Grant No. 164100510007 and CXTD2015018) and Zhengzhou University (Grant No. 1421316035 & 2016xjxm258).

Author Contributions: Liwei Mi and Weihua Chen conceived and designed the experiments; Nannan Wang performed the experiments and wrote the paper; Shizhong Cui and Wutao Wei analyzed the data and designed the figures of manuscript; Hongwei Hou rechecked the manuscript.

Conflicts of Interest: The authors declare no conflict of interest.

References

1. Fowler,J.D.; Allen, M.J.; Tung, V.C.; Yang, Y.; Kaner,R.B.; Weiller,B.H. Practical Chemical Sensors from Chemically Derived Graphene.*ACS Nano***2009**,*3*, 301−306.[CrossRef][PubMed]
2. Mohan,D.; Singh,K.P. Single- and Multi-Component Adsorption of Cadmium and Zinc Using Activated Carbon Derived from Bagasse--an Agricultural Waste.*Water Res.***2002**,*36*, 2304−2318.[CrossRef][PubMed]
3. Wei,W.;Ma,G.H.;Hu, G.;Yu, D.;Mcleish, T.;Su,Z.G.;Shen, Z.Y.Preparation of Hierarchical Hollow $CaCO_3$ Particles and the Application as Anticancer Drug Carrier.*J. Am. Chem. Soc.***2008**, *130*, 15808–15810.[CrossRef][PubMed]
4. Wang,J.; Timchalk,C.; Lin,Y.H.Carbon Nanotube-Based Electrochemical Sensor for Assay of Salivary Cholinesterase Enzyme Activity: An Exposure Biomarker of Organophosphate Pesticides and Nerve Agents.*Environ. Sci. Technol.***2008**,*42*, 2688−2693.[CrossRef][PubMed]
5. Frackowiak, E.; Béguin, F. Carbon Materials for the Electrochemical Storage of Energy in Capacitors. *Carbon***2001**,*39*, 937−950.[CrossRef]
6. Zhu,Y.W.; Murali,S.; Stoller,M.D.; Ganesh,K.J.; Cai,W.W.; Ferreira,P.J.; Pirkle, A.; Wallace,R.M.; Cychosz,K.A.; Thommes,M.; Su, D.; Stach, E.A.; Ruoff, R.S.Carbon-Based Supercapacitors Produced by Activation of Graphene.*Science***2011**, *332*, 1537–1541.[CrossRef][PubMed]
7. Sun,J.K.; Xu,Q. Functional materials derived from open framework templates/precursors: synthesis and applications.*Energy Environ. Sci.***2014**,*7*, 2071–2100.
8. Pandolfo, A.G.; Hollenkamp, A.F. Carbon Properties and Their Role in Supercapacitors. *J. Power. Sources***2006**, *157*, 11−27.[CrossRef]
9. Zhang, L.L.; Zhao, Z.S. Carbon-Based Materials as Supercapacitor Electrodes. *Chem. Soc. Rev.***2009**, *38*, 2520–2531.[CrossRef]
10. Di, J.T.; Hu, D.M.; Chen, H.Y.; Yong, Z.Z.; Chen, M.H.; Feng, Z.H.; Zhu, Y.T.; Li, Q.W. Ultrastrong, Foldable, and Highly Conductive Carbon Nanotube Film.*ACS nano***2012**, *6*, 5457–5464.[CrossRef][PubMed]
11. Zhao, J.; Zheng, Q.J.; Petek, H.;Yang, J.L. Nonnuclear Nearly Free Electron Conduction Channels Induced by Doping Charge in Nanotube–Molecular Sheet Composites. *J. Phys. Chem. A***2014**, *118*, 7255–7260.[CrossRef][PubMed]
12. Kim, J.H.;Lee, K.H.; Overzet, L. J.;Lee, G.S. Synthesis and Electrochemical Properties of Spin-Capable Carbon Nanotube Sheet/MnO_x Composites for High-Performance Energy Storage Devices. *Nano Lett.* **2011**, *11*, 2611–2617.[CrossRef]
13. Sanchez, D.V.P.;Huynh, P.;Kozlov, M.E.;Baughman, R.H.;Vidic, R.D.;Yun, M. Carbon Nanotube/Platinum (Pt) Sheet as an Improved Cathode for Microbial Fuel Cells.*Energy Fuels* **2010**, *24*, 5897–5902.[CrossRef]
14. Xu, X.; Li, H.;Zhang, Q.Q.;Hu, H.;Zhao, Z.B.;Li, J.H.;Li, J.Y.;Qiao, Y.;Gogotsi, Y. Self-Sensing, Ultralight, and Conductive 3D Graphene/Iron Oxide Aerogel Elastomer Deformable in a Magnetic Field.*ACS nano***2015**, *9*, 3969–3977.[CrossRef][PubMed]

15. Wang, X.W.;Sun, G.Z.;Routh, P.;Kim, D.H.;Huang, W.;Chen, P. Heteroatom-Doped Graphene Materials: Syntheses, Properties and Applications.*Chem. Soc. Rev.***2014**, *43*, 7067−7098.[CrossRef][PubMed]
16. Luo, H.X.;Liu, Z.Y.;Chao, L.M.;Wu, X.C.;Lei, X.D.;Chang, Z.;Sun, X.M. Synthesis of Hierarchical Porous N-Doped Sandwich-Type Carbon Composites as High Performance Supercapacitor Electrodes.*J. Mater. Chem. A.***2015**, *3*, 3667–3675.[CrossRef]
17. He, S.J.;Chen, W. 3D Graphene Nanomaterials for Binder-Free Supercapacitors: Scientific Design for Enhanced Performance. *Nanoscale***2015**, *7*, 6957–6990.[CrossRef][PubMed]
18. Zhai, S.L.;Jiang, W.C.;Wei, L.;Karahan, H.E.;Yuan, Y.;Ng, A.K.;Chen, Y. All-Carbon Solid-State Yarn Supercapacitors from Activated Carbon and Carbon Fibers for Smart Textiles.*Mater. Horiz.* **2015**, *2*, 598–605. [CrossRef]
19. Kang, E.;Jeon, G.;Kim, J.K.Free-Standing, Well-Aligned Ordered Mesoporous Carbon Nanofibers on Current Collectors for High-Power Micro-Supercapacitors.*Chem. Commun.* **2013**, *49*, 6406−6408.[CrossRef][PubMed]
20. Sun, G.Z.;Zhang, X.;Lin, R.Z.;Yang, J.;Zhang, H.;Chen, P. Hybrid Fibers Made of Molybdenum Disulfide, Reduced Graphene Oxide, and Multi-Walled Carbon Nanotubes for Solid-State, Flexible, Asymmetric Supercapacitors.*Angew. Chem. Int. Edit.***2015**, *54*, 46651-46656.[CrossRef][PubMed]
21. Huang, J.L.;Wang, J.Y.;Wang, C.W.;Zhang, H.N.;Lu, C.X.;Wang, J.Z. Hierarchical Porous Graphene Carbon-Based Supercapacitors.*Chem. Mater.***2015**, *27*, 2107-2113.[CrossRef]
22. Cherusseri, J.; Kar, K.K. Hierarchically Mesoporous Carbon Nanopetal Based Electrodes for Flexible Supercapacitors with Super-Long Cyclic Stability. *J. Mater. Chem. A***2015**, *3*, 21586–21598.[CrossRef]
23. Jin, F.Y.; Xiao, S.; Lu, L.J.; Wang, Y. Efficient Activation of High-Loading Sulfur by Small CNTs Confined Inside a Large CNT for High-Capacity and High-Rate Lithium−Sulfur Batteries.*Nano Lett.* **2016**, *16*, 440-447.[CrossRef][PubMed]
24. Wang, Y.; Wu, M.H.; Jiao, Z.; Lee, J.Y. Sn@CNT and Sn@C@CNT nanostructures for superior reversible lithium ion storage. *Chem. Mater.* **2009**, *21*, 3210-3215.[CrossRef]
25. Yu, Z.N.;Tetard, L.;Zhai, L.;Thomas, J.Y. Supercapacitor electrode materials: nanostructures from 0 to 3 dimensions.*Energy Environ. Sci.* **2015**, *8*, 702-730.[CrossRef]
26. Huang, X.;Yin, Z.Y.;Wu, S.X.;Qi, X.Y.;He, Q.Y.;Zhang, Q.C.;Yan, Q.Y.;Boey, F.; Zhang, H.Graphene-Based Materials: Synthesis, Characterization, Properties, and Applications.*Small* **2011**, *7*, 1876-1902.[CrossRef][PubMed]
27. Oraon, R.;Adhikari, A.D.;Tikari, S.K.;Nayak, G.C. Nanoclay Based Hierarchical Interconnected Mesoporous CNT/PPy Electrode with Improved Specific Capacitance for High Performance Supercapacitor.*Dalton, Trans.* **2016**, *45*, 9113–9126.[CrossRef]
28. Stoller, M.D.;Park, S.J.;Zhu, Y.W.;An, J.;Ruoff, R.S. Graphene-Based Ultracapacitors.*Nano Lett.* **2008**, *8*, 3498-3502.[CrossRef]
29. Zhang, X.M.;Jiao, Y.Q.;Sun, L.;Wang, L.;Wu, A.P.;Yan, H.J.;Meng, M.C.;Tian, C.G.;Jiang, B.J.;Fu, H.G. GO-induced assembly of gelatin toward stacked layer-like porous carbon for advanced supercapacitors.*Nanoscale***2016**, *8*, 2418–2427.[CrossRef][PubMed]
30. W.J. Zhou, X.H. Cao, Z.Y. Zeng, W.H. Shi, Y.Y. Zhu, Q.Y. Yan, H. Liu, J.Y. Wang, H. Zhang, One-Step Synthesis of Ni_3S_2 Nanorod@$Ni(OH)_2$ Nanosheet Core–Shell Nanostructures on a Three-dimensional Graphene Network for High-Performance Supercapacitors, *Energy Environ. Sci.* **2013**, *6*, 2216–2221.[CrossRef]
31. Zhang, S.T.;Zheng, M.B.;Lin, Z.X.;Li, N.W.;Liu, Y.J.;Zhao, B.;Pang, H.;Cao, J.M.;He, P.;Shi, Y. Activated Carbon with Ultrahigh Specific Surface Area Synthesized from Natural Plant Material for Lithium–Sulfur Batteries. *J. Mater. Chem. A* **2014**, *2*, 15889–15896.[CrossRef]
32. Zhu, C.Y.;Akiyama, T. Cotton Derived Porous Carbon via an MgO Template Method for High Performance Lithium Ion Battery Anodes. *Green Chem.* **2016**, *18*, 2106–2114.[CrossRef]
33. Wang, L.;Zhang, Q.Y.;Chen, S.L.;Xu, F.G.;Chen, S.H.; Jia, J.B.;Tan, H.L.;Hou, H.Q.;Song, Y.H. Electrochemical Sensing and Biosensing Platform Based on Biomass-Derived Macroporous Carbon Materials.*Anal. Chem.* **2014**, *86*, 1414–1421.[CrossRef][PubMed]
34. Cheng, P.;Li, T.;Yu, H.;Zhi, L.;Liu, Z.H.;Lei, Z.B. Biomass-Derived Carbon Fiber Aerogel as a Binder-Free Electrode for High-Rate Supercapacitors. *J. Phys. Chem. C* **2016**, *120*,2079–2086.[CrossRef]

35. Chen, H.;Liu, D.;Shen, Z.H.;Bao, B.F.;Zhao, S.Y.;Wu, L.M. Functional Biomass Carbons with Hierarchical Porous Structure for Supercapacitor Electrode Materials.*Electrochim. Acta* **2015**, *180*,241–251.[CrossRef]
36. Hou, J.H.;Cao, C.B.;Idrees, F.;Ma, X.L. Hierarchical Porous Nitrogen-Doped Carbon Nanosheets Derived from Silk for Ultrahigh-Capacity Battery Anodes and Supercapacitors.*ACS Nano* **2015**, *9*, 2556–2564.[CrossRef][PubMed]
37. Yang, X.X.;Li, M.;Guo, N.N.;Yan, M.;Yang, R.;Wang, F. Functionalized Porous Carbon with Appropriate Pore Size Distribution and Open Hole Texture Prepared by H_2O_2 and EDTA-2Na Treatment of Loofa Sponge and Its Excellent Performance for Supercapacitors.*RSC Adv.* **2016**, *6*, 4365–4376.[CrossRef]
38. Wang, H.Q.;Chen, Z.X.;Liu, H.K.;Guo, Z.P. A Facile Synthesis Approach to Micro–Macroporous Carbon from Cotton and Its Application in the Lithium–Sulfur Battery.*RSC Adv.* **2014**, *4*, 65074–65080.[CrossRef]
39. Kim, M.H.;Kim, K.B.;Park, S.M.;Roh, K.C.;Hierarchically Structured Activated Carbon for Ultracapacitors.*Sci. Rep.* **2016**, *6*, 21182–21187.[CrossRef][PubMed]
40. Sun, L.;Tian, C.G.;Fu, Y.;Yang, Y.; Yin, J.;Wang, L.;Fu, H.G. Nitrogen-Doped Porous Graphitic Carbon as an Excellent Electrode Material for Advanced Supercapacitors.*Chem. Eur. J.* **2014**, *20*, 564–574.[CrossRef][PubMed]
41. Liu, D.;Yu, S.;Shen, Y.L.;Chen, H.;Shen, Z.H.;Shen, S.Y.;Zhao, S.Y.;Fu, S.Y.;Yu, Y.M.;Bao, B.F.;Polyaniline Coated Boron Doped Biomass Derived Porous Carbon Composites for Supercapacitor Electrode Materials. *Ind. Eng. Chem. Res.* **2015**, *54*, 12570–12579.[CrossRef]
42. Gao, S.Y.;Chen, Y.L.;Fan, H.;Wei, X.J.;Hu, C.G.;Luo, H.X.;Qu, L.T. Large Scale Production of Biomass-Derived N-Doped Porous Carbon Spheres for Oxygen Reduction and Supercapacitors.*J. Mater. Chem. A.* **2014**, *2*, 3317–3324. [CrossRef]
43. Raymundo-Piñero, E.;Leroux, F.;Béguin, F. A High-Performance Carbon for Supcapacitors Obtained by Carbonization of a Seaweed Biopolymer.*Adv. Mater.* **2006**, *18*, 1877–1882.[CrossRef]
44. Qie, L.;Chen, W.M.;Xu, H.H.;Xiong, X.Q.;Jiang, Y.;Zou, F.;Hu, X.L.;Lin, Y.;Zhang, Z.L.;Huang, Y.H. Synthesis of Functionalized 3D Hierarchical Porous Carbon for High-Performance Supercapacitors.*Energy Environ. Sci.* **2013**, *6*, 2497–2504.[CrossRef]
45. Li, Z.;Zhang, L.;Amirkhiz, B.S.;Tan, X.H.;Xu, Z.W.;Wang, H.L.;Olsen, B.C.;Holt, C.M.B.;Mitlin, D. Carbonized Chicken Eggshell Membranes with 3D Architectures as High-Performance Electrode Materials for Supercapacitors.*Adv. Energy Mater.* **2012**, *2*, 431–437.[CrossRef]
46. Niu, Z.Q.;Zhou, W.Y.;Chen, X.D.;Chen, J.;Xie, S.S. Highly Compressible and All-Solid-State Supercapacitors Based on Nanostructured Composite Sponge.*Adv. Mater.* **2015**, *27*,6002–6008.[CrossRef][PubMed]
47. Jain, A.;Aravindan, V.;Jayaraman, S.;Kumar, P.S.;Balasubramanian, R.;Ramakrishna, S.;Madhavi, S.;Srinivasan, M.P. Activated carbons derived from coconut shells as high energy density cathode material for Li-ion capacitors.*Sci. Rep.* **2013**, *3*, 3002–3007.[CrossRef][PubMed]
48. Li, Y.Z.;Zhang, Q.H.;Zhang, J.X.;Jin, L.;Zhao, X.;Xu,T. A top-down approach for fabricating free-standing bio-carbon supercapacitor electrodes with a hierarchical structure.*Sci. Rep.* **2015**, *5*,14155–14164.[CrossRef][PubMed]

Sample Availability: Samples of the compoundsare available from the authors.